

## Al<sub>2</sub>O<sub>3</sub>-C<sub>act</sub>-(CuO, Cr<sub>2</sub>O<sub>3</sub>, Co<sub>3</sub>O<sub>4</sub>) Adsorbents-Catalysts: Preparation and Characterization

Gitana DABRILAITĖ-KUDŽMIENĖ\*, Saulius KITRYS

Department of Physical Chemistry, Faculty of Chemical Technology, Kaunas University of Technology, Radvilėnų pl. 19, LT-50254, Kaunas, Lithuania

crossref <http://dx.doi.org/10.5755/j01.ms.19.1.3832>

Received 18 October 2011; accepted 21 March 2012

Al<sub>2</sub>O<sub>3</sub>-C<sub>act</sub>-(CuO, Cr<sub>2</sub>O<sub>3</sub>, Co<sub>3</sub>O<sub>4</sub>) adsorbents-catalysts were prepared using Al<sub>2</sub>O<sub>3</sub>-C<sub>act</sub> (alumina gel-activated carbon) adsorbent and different amount of CuO, Cr<sub>2</sub>O<sub>3</sub> and Co<sub>3</sub>O<sub>4</sub>. The active components were incorporated into wet alumina gel-carbon mixture using different conditions (by sol-gel method and mixing a milled metal oxides). Equilibrium adsorptive capacity measurements of alcohol vapours were carried out in order to determine the influence of preparation conditions on the stability of prepared adsorbents-catalysts. Specific surface area of the prepared adsorbents-catalysts were measured by BET method. It was established that for adsorbent-catalyst produced by sol-gel method  $S_{BET} = 244.7$  m<sup>2</sup>/g. Surface area  $S_{BET} = 29.32$  m<sup>2</sup>/g was obtained for adsorbent-catalyst with metal oxides. On the basis of these results it was assumed that active carbon was lost in this adsorbent-catalyst during the preparation process. Sol-gel derived adsorbent-catalyst was tested for the oxidation of methanol vapours. Catalytic oxidation was carried out in fixed-bed reactor. Experimental data indicate that adsorptive capacity of the adsorbent-catalyst is (3.232–3.259) mg/m<sup>3</sup> CH<sub>3</sub>OH at relative air humidity is 40%–50%. During a fast heating of CH<sub>3</sub>OH-saturated adsorbent-catalyst a part of adsorbate is converted to CO<sub>2</sub> and H<sub>2</sub>O. Methanol conversion increases with increasing of adsorbent-catalyst heating rate.

*Keywords:* activated carbon, adsorbent-catalyst, metal oxides, oxidation, methanol.

### 1. INTRODUCTION

The spectrum of activated carbon applications for catalysis and adsorption is very wide. This is determined by carbon's ability to activate reactive substances. On the surface of carbon, radical centers ("trivalent carbon") are located, which catalyze various oxidation and reduction processes. Typical examples of carbon-catalyzed processes are chlorination (CO, SO<sub>2</sub>, C<sub>2</sub>H<sub>2</sub>), dehydrochlorination (C<sub>2</sub>H<sub>2</sub>Cl<sub>4</sub>), oxidation (H<sub>2</sub>S, SO<sub>2</sub>, NO), dehydration (C<sub>2</sub>H<sub>5</sub>OH, HCOOH), dissociation (H<sub>2</sub>O<sub>2</sub>) [1–10]. However, as mentioned before, the possibility of much greater use of activated carbon opens up when metals or various metal compounds are dispersed on the surface of carbon. In addition to the platinum-group metals, oxides of variable valence metals (Ni, Cu, Co, Mn, Cr) are the most active components of catalysts used for oxidation of organic compounds [11–20]. Interaction between oxygen molecules and oxide surface leads to formation of various oxygen radicals which react with organic molecules.

The usage of activated carbons as catalysts support is determined not only by the properties mentioned before but also by the high specific surface area and high adsorption capacity for adsorptive vapour, low selectivity and suitability for work in wet environments, relatively low cost, etc. However, in addition to those mentioned positive properties of activated carbon, they also have some limitations. In the presence of oxygen or other oxidizers their thermal resistance is reduced. Also, activated carbons are microporous what limits the transportation of adsorbates towards the active components.

Because of its abundance and low cost as well as excellent physical and chemical properties aluminum oxide is also very often used as a catalyst support [16, 21–25]. It is heat-resistant adsorbent with large transport pores. It is likely that alumina and activated carbon derivatives can be the basis for catalysts, where micro inserts of activated carbon perform the role of adsorbent and wide pore alumina part acts like a tray for catalysts active components. In order to produce heat resistant catalyst, we wanted to find the way to prevent a direct contact of activated carbons and alumina. Our previously produced alumina gel and activated carbons derivatives were more thermoresistant than pure activated carbons. In addition, 5 (weight) % additive of activated carbon highly increased the specific surface of alumina gel and slowed down the adsorption of water vapour on the surface of adsorbent [26]. Alumina and activated carbons derivatives can be used as adsorbents or as the base for catalyst. For the synthesis of adsorbents-catalysts as active components Cu, Cr and Co oxides were chosen: CuO as the most active oxide for VOC oxidation, Cr<sub>2</sub>O<sub>3</sub> as additive which increases thermal resistance and activity of copper (mostly, if CuCr<sub>2</sub>O<sub>4</sub> is formed during synthesis), Co<sub>3</sub>O<sub>4</sub> as additive, which increases catalysts resistance to poisons.

### 2. EXPERIMENTAL

**Preparation of adsorbent-catalyst.** Al<sub>2</sub>O<sub>3</sub>-C<sub>act</sub>-(CuO, Cr<sub>2</sub>O<sub>3</sub>, Co<sub>3</sub>O<sub>4</sub>) adsorbents-catalysts were prepared as composites by adding various amounts of active components (Cu, Cr, Co gels (hydroxides) or oxides) into humid mixture of alumina gel and WS-42A type (Chemviron Carbon, Germany) activated carbon (5% wt.) [26]. We tried to immobilize active components of adsorbent-catalyst by these methods:

\*Corresponding author. Tel.: +370-686-65420; fax.: +370-37-300152. E-mail address: [gitana.dabrilaitė@ktu.lt](mailto:gitana.dabrilaitė@ktu.lt) (G. Dabrilaitė-Kudžmienė)



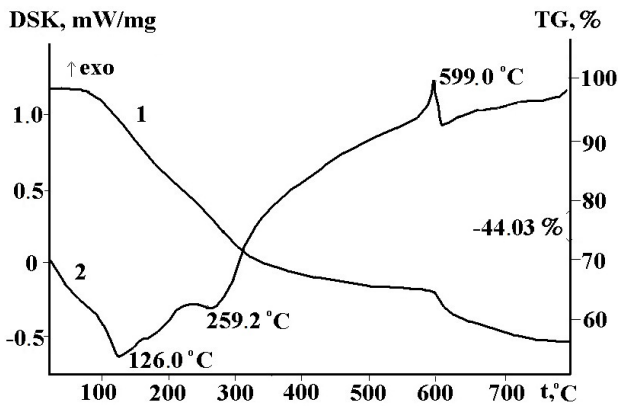


**Fig. 2.** Curves of thermal analysis of humid  $\text{Al}_2\text{O}_3\text{-C}_{\text{act}}\text{-(CuO, Cr}_2\text{O}_3, \text{Co}_3\text{O}_4)$  adsorbent-catalyst produced using the gels of metal hydroxides:  
1 – Thermogravimetry (TG);  
2 – Differential Scanning Calorimetry (DSC)

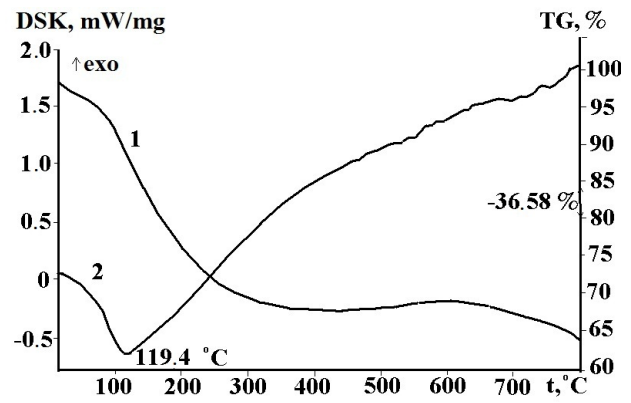


**Fig. 3.** Curves of thermal analysis of humid  $\text{Al}_2\text{O}_3\text{-C}_{\text{act}}\text{-(CuO, Cr}_2\text{O}_3, \text{Co}_3\text{O}_4)$  adsorbent-catalyst produced using the powders of metal oxides:  
1 – Thermogravimetry (TG);  
2 – Differential Scanning Calorimetry (DSC)

and boehmite ( $\text{AlO}(\text{OH})$ ).

Thermal analysis of humid samples showed that catalysts lose water at  $\sim 120^\circ\text{C}$  (Fig. 2). The endothermic effect at  $250^\circ\text{C} - 260^\circ\text{C}$  is attributed to thermal dissociation of metal hydroxides [32]. The exothermic effect above  $580^\circ\text{C}$  showed the destruction of catalyst structure. The endothermic effect due to evaporation of water was found at  $\sim 120^\circ\text{C}$  for catalysts produced by adding the powder of metal oxides (Fig. 3). TG curve falls consecutively, and that of DSC rises if temperature is increased. This lets to assume that metal oxides can be slowly reduced by activated carbon.

In order to confirm this assumption, we performed preliminary tests for both obtained adsorbent-catalysts according to their equilibrium adsorption capacity (Table 1). The results of these measurements show that adsorption capacities increase only for adsorbent-catalyst which is produced by adding gel type metals hydroxides. If metal oxides are added in the form of powder, the

adsorption capacity of thermally treated adsorbent-catalyst is significantly lower.

This shows that during thermal treatment of humid catalysts, when using powdery oxides, activated carbon becomes oxidized (due to their direct contact). In this case one obtains  $\text{Al}_2\text{O}_3\text{-C}_{\text{act}}\text{-metal oxide}$  catalysts having small specific surface area. These assumptions were confirmed by BET measurements for catalyst having  $\text{CuO}$ ,  $\text{Cr}_2\text{O}_3$  and  $\text{Co}_3\text{O}_4$  powders. The calculated  $S_{\text{BET}}$  value was  $29.32 \text{ m}^2/\text{g}$ , which is close to that for macroporous  $\text{Al}_2\text{O}_3$  ( $S_{\text{BET}} = 30.7 \text{ m}^2/\text{g}$ ) [33]. Adsorbent-catalyst prepared from gels  $S_{\text{BET}} = 244.7 \text{ m}^2/\text{g}$  is nearly equal to  $\text{Al}_2\text{O}_3\text{-C}_{\text{act}}$  by specific surface area ( $S_{\text{BET}} = 280.43 \text{ m}^2/\text{g}$ ).

The experimental results were validated by findings of thermodynamic calculations (Table 2). By comparing the standard Gibbs potentials ( $\Delta_r G_T^0$ ) it can be noticed that all reactions, except (3), can be proceeded at low temperatures, and carbon inserts remain intact at high temperatures only if no contact with metal oxides is present.

**Table 1.** Adsorption equilibrium capacity for methanol and isobutanol vapors at  $25^\circ\text{C}$  and (748 – 756) mm Hg

Composites	The amount of adsorbed methanol $\sum X_{\text{met}}^p$ , mg/g	The amount of adsorbed isobutanol $\sum X_{\text{but}}^p$ , mg/g
$\text{Al}_2\text{O}_3\text{-C}_{\text{akt}}$	61.4	34.3
$\text{Al}_2\text{O}_3\text{-C}_{\text{akt}}\text{-(CuO, Cr}_2\text{O}_3, \text{Co}_3\text{O}_4)$ prepared from gels	111.1	59.5
$\text{Al}_2\text{O}_3\text{-C}_{\text{akt}}\text{-(CuO, Cr}_2\text{O}_3, \text{Co}_3\text{O}_4)$ prepared from oxides	8.6	5.2

**Table 2.** Standard Gibbs potentials of reactions

Reactions	$\Delta_r G_T^0$ , kJ/mol at various temperatures $t$ , $^\circ\text{C}$						
	100	200	300	400	500	600	800
$\text{C} + \text{O}_2 \rightarrow \text{CO}_2$ (1)	-398.2	-396.5	-395.7	-395.4	-395.2	-395.1	-394.7
$\text{C} + \frac{1}{2} \text{O}_2 \rightarrow \text{CO}$ (2)	-153.3	-156.4	-163.5	-171.3	-179.4	-187.5	-204.1
$\text{C} + \text{H}_2\text{O} \rightarrow \text{H}_2 + \text{CO}$ (3)	73.5	64.5	52.1	39.0	25.5	11.9	-18.5
$\text{C} + \text{CuO} \rightarrow \text{Cu} + \text{CO}$ (4)	-29.8	-41.2	-55.0	-67.1	-80.0	-92.3	-117.2
$\text{C} + 2\text{CuO} \rightarrow \text{Cu}_2\text{O} + 2\text{CO}$ (5)	-243.2	-271.8	-299.6	-327.9	-355.8	-384.0	-436.9



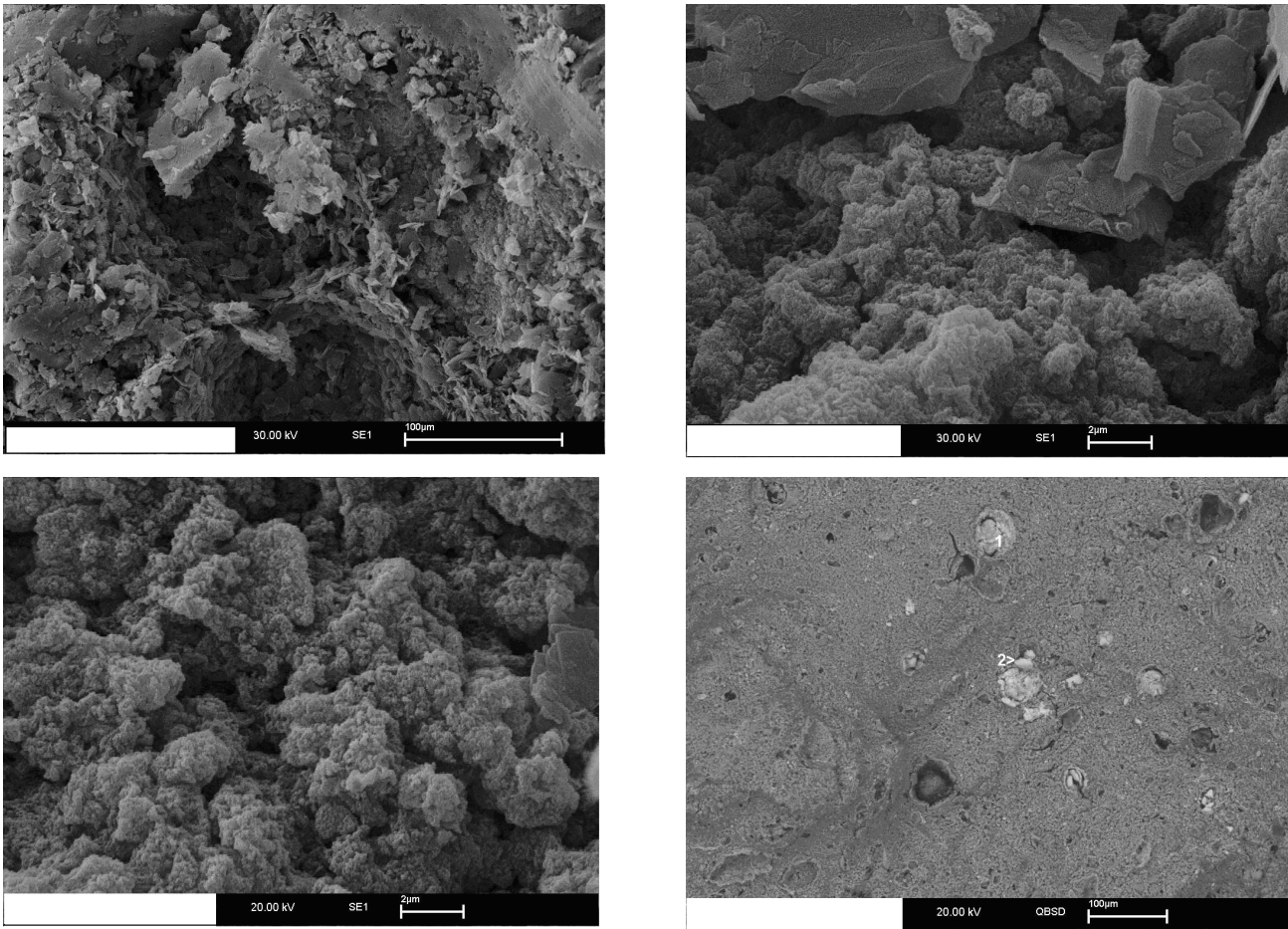


Fig. 4. SEM images of  $\text{Al}_2\text{O}_3\text{-C}_{\text{act}}\text{-(CuO, Cr}_2\text{O}_3, \text{Co}_3\text{O}_4)$  adsorbent-catalyst prepared by using gel-type hydroxides at different scales

On the basis of these results, for further investigations adsorbent-catalyst prepared by using gel-type hydroxides was used. Such adsorbent-catalyst is characterized by sufficient thermal stability and had a high specific surface area, which is influenced by activated carbon additive. These properties are determined by the fact, that using our synthesis method when adding gel type metal hydroxides into  $\text{Al}_2\text{O}_3\text{-C}_{\text{act}}$  gel type composite, metal oxides are localized in the porous alumina gel and do not make a direct contact with activated carbon (Fig. 4).

**Specific surface area and pore structure.**  $\text{Al}_2\text{O}_3\text{-C}_{\text{act}}\text{-(CuO, Cr}_2\text{O}_3, \text{Co}_3\text{O}_4)$  adsorbent-catalyst was chosen for the detailed examination of specific surface.

Calculations of specific surface area ( $S_{\text{BET}}$ ) were performed by using primary part of  $\text{N}_2$  adsorption-desorption hysteresis when  $p/p_0 < 0.30$  (Fig. 5) [34].

Clear arch is seen in isotherms of hysteresis (point A), which shows that  $\text{N}_2$  monomolecular layer has formed. By plotting  $1/X(p/p_0) - 1$  as a function of  $p/p_0$ , linear BET plots are obtained (Fig. 6), and their reliability coefficient  $R^2$  is 0.9993.

As noticed, specific surface area for adsorbent-catalyst is  $S_{\text{BET}} = 244.7 \text{ m}^2/\text{g}$  (for  $\text{Al}_2\text{O}_3$   $S_{\text{BET}} = 30.7 \text{ m}^2/\text{g}$ , for  $\text{Al}_2\text{O}_3\text{-C}_{\text{act}}$   $S_{\text{BET}} = 280.4 \text{ m}^2/\text{g}$  [33]).  $C_{\text{BET}}$  constant value is calculated to be 168.7 and that allows to evaluate validity of BET measurements (Table 3). It is known that the most accurate results of  $S_{\text{BET}}$  are obtained when  $C_{\text{BET}}$  is 50–250. In our case, the calculated high values of  $C_{\text{BET}}$  were conditioned by additive of microporous activated carbon.

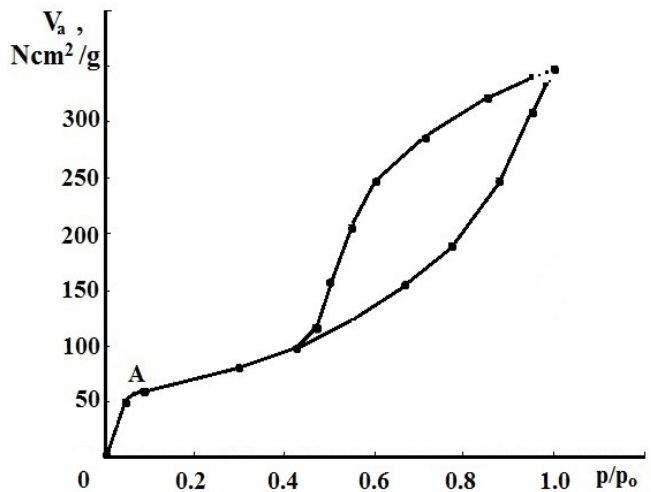


Fig. 5.  $\text{N}_2$  adsorption-desorption isotherms at 77 K for adsorbent-catalyst

Table 3. Calculated parameters of specific surface area ( $S_{\text{BET}}$ )

BET equation constants		Capacity of monolayer $X_m = \frac{1}{S+I}$ , g	Specific surface area $S_{\text{BET}}$ , $\text{m}^2/\text{g}$	Constant $C_{\text{BET}} = \frac{1}{I \cdot X_m}$
Slope, $tg \alpha = S$	Intercept, $I$			
3053.3	17.97	0.00033	244.7	168.7

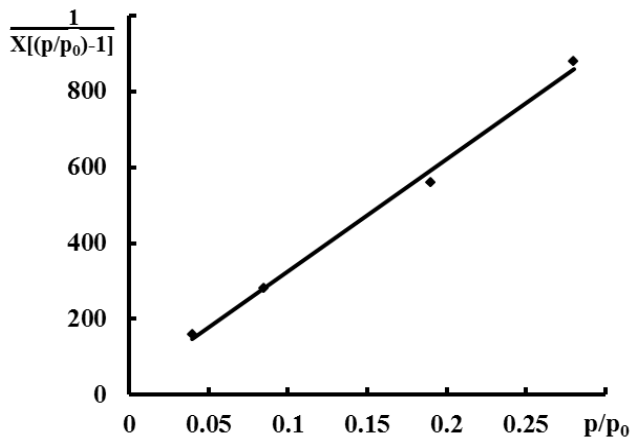


Fig. 6. N<sub>2</sub> adsorption isotherm at 77 K in BET plot

It is possible to forecast the pore form of adsorbents according to de Boer classification [35] of hysteresis isotherms (Fig. 5). Spherical forms of pores prevail in the catalyst: when  $p/p_0 = 0.6-0.95$  the broad part of hysteresis isotherm can be seen, and when  $p/p_0$  decreases down to 0.4, the phenomenon of hysteresis ends. This approximate evaluation of the form of pores is supported by the comparison of  $S_{BET}$  results with the total specific surface  $\Sigma A$ , calculated according to scheme of C. Orr, J. M. Dalla Valle [36]. It has been determined that  $S_{BET} = 244.7 \text{ m}^2/\text{g}$ , and  $\Sigma A = 502.98 \text{ m}^2/\text{g}$ . The results show that regarding the form of pores the polydispersial structure is typical for catalyst when the slit-like pores are supplemented by the capillaries of bigger radius. These assumptions are confirmed by the calculations of integral and differential distribution of pores according to their diameters. The pores of 1.8 nm–2.0 nm and 2.4 nm–2.7 nm radius prevails catalyst, mean radius of pores  $\bar{r}_p = 2.6 \text{ nm}$  (for  $\text{Al}_2\text{O}_3$   $\bar{r}_p = 3.2 \text{ nm}$ , for  $\text{Al}_2\text{O}_3\text{-C}_{act}$   $\bar{r}_p = 2.0 \text{ nm}$ ), total volume of pores  $\Sigma V_p = 0.652 \text{ cm}^3/\text{g}$  (for  $\text{Al}_2\text{O}_3$   $\Sigma V_p = 0.118 \text{ cm}^3/\text{g}$ , for  $\text{Al}_2\text{O}_3\text{-C}_{act}$   $\Sigma V_p = 0.332 \text{ cm}^3/\text{g}$ ).

**Activity of  $\text{Al}_2\text{O}_3\text{-C}_{act}$ -(CuO, Cr<sub>2</sub>O<sub>3</sub>, Co<sub>3</sub>O<sub>4</sub>) adsorbent-catalyst.** It is customary to test an activity of VOC oxidation catalysts in CO or alcohol oxidation reactions. Exception is made by catalysts acting at high (>550 °C) temperatures, which are tested towards cyclic hydrocarbon (mostly benzene) oxidation.

We tested  $\text{Al}_2\text{O}_3\text{-C}_{act}$ -(CuO, Cr<sub>2</sub>O<sub>3</sub>, Co<sub>3</sub>O<sub>4</sub>) catalyst activity in methanol vapour oxidation using two technologies:

- 1) at constant temperature of catalyst bed;
- 2) in the cyclic adsorptive-catalytic process.

We maintained the methanol concentration at inlet gas to be 800 mg/Nm<sup>3</sup>. Inlet mixture humidity was equal to relative air humidity and varied in the range of 40 %–50 % (8–12 g/Nm<sup>3</sup>). As inlet mixture CH<sub>3</sub>OH is constantly supplied, methanol vapour reaction with air oxygen starts when average temperature in adsorbent-catalyst load reaches 100 °C. As temperature rises, methanol oxidation degree increases up to 92.2 % at 370 °C (Fig. 7).

When temperature of flow of methanol vapour – humid air mixture reaches 150 °C–300 °C, methanol is oxidized not only to CO<sub>2</sub> and H<sub>2</sub>O, but also into intermediate oxidation product formaldehyde (Fig. 8).

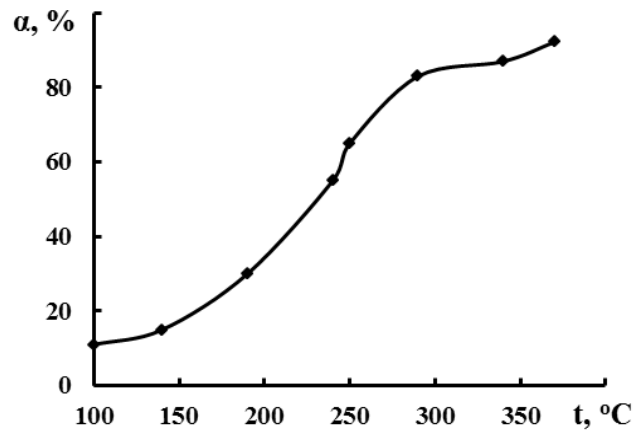


Fig. 7. Dependence of methanol oxidation degree on temperature

The largest quantity of formaldehyde (~100 mg/Nm<sup>3</sup>) is formed when average temperature of adsorbent-catalyst bed is 235 °C. As temperature increases above 235 °C, formaldehyde concentration decreases. At 350 °C formaldehyde is not found. This indicates that the process proceeds according to the well known parallel-consecutive mechanism of oxidation [37].

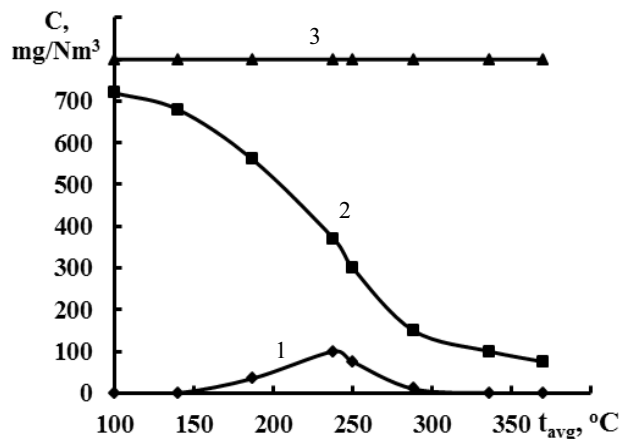


Fig. 8. Dependence of methanol and formaldehyde concentrations in exit gases at an average temperature of adsorbent-catalyst bed (linear flow rate is 0.088 m/s): 1 – CH<sub>2</sub>O; 2 – CH<sub>3</sub>OH; 3 – CH<sub>3</sub>OH concentration in inlet gas

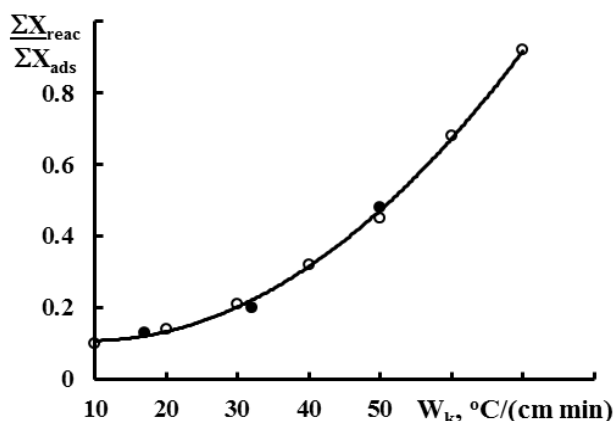
The activity of  $\text{Al}_2\text{O}_3\text{-C}_{act}$ -(CuO, Cr<sub>2</sub>O<sub>3</sub>, Co<sub>3</sub>O<sub>4</sub>) adsorbent-catalyst was also investigated in the cyclic adsorptive-catalytic oxidation process of methanol vapour. Firstly, adsorbent-catalyst bed was saturated with methanol vapour at 25 °C–30 °C. Dynamic adsorption capacity of adsorbent-catalysts  $\Sigma X_{CH_3OH}$  was found to be (3.232–3.259) mg/cm<sup>3</sup>.

When the load of adsorbent-catalyst, saturated with methanol vapour, is quickly heated by a flow of hot air (320 °C–525 °C), methanol conversion into CO<sub>2</sub> and H<sub>2</sub>O occurs (Table 4). This indicates that if the linear flow rate of hot air is 0.088 m/s and if the heating rate of beds upper layer is 50 °C/(cm·min), methanol vapour oxidation degree is  $\alpha = 47.4 \%$ . Formaldehyde is formed (0.055 mg/cm<sup>3</sup>) only when regenerating the bed with air flow of 320 °C and slowly heating the catalyst. Under our experimental conditions we did not find formaldehyde upon fast heating.

**Table 4.** Dependence of adsorptive-catalytic oxidation degree on the rate of temperature rise

Adsorption time, min	Initial concentration of methanol vapour, mg/Nm <sup>3</sup>	Amount of adsorbed CH <sub>3</sub> OH $\Sigma X_{ads}$ , mg/cm <sup>3</sup>	Heating rate $w_k$ of upper layer of catalyst bed °C/(cm·min)	Regeneration time, min	Regenerated CH <sub>3</sub> OH quantity $\Sigma X_{reg}$ , mg/cm <sup>3</sup>	CH <sub>3</sub> OH oxidation degree $\alpha$ , %
90	851.67	3.247	17.3	42	2.827	12.9
90	842.00	3.232	32.3	38	2.591	19.8
90	856.15	3.259	50.0	32	1.713	47.4

The quantities of methanol converted to CO<sub>2</sub> and H<sub>2</sub>O vapour or desorbed depend on heating rate of catalyst bed in post-reactive gas (Fig. 9). As the heating rate of catalyst load increases, the fraction of reacted CH<sub>3</sub>OH increases too.

**Fig. 9.** Dependence of conversion degree and heating rate of adsorbent-catalyst bed (• – experimental, ◦ – calculated)

The obtained results can be described by the equation:

$$\frac{\Sigma X_{\text{reac}}}{\Sigma X_{\text{ads}}} = 0.0609 e^{0.04 W_k}, \quad (\Sigma X_{\text{reac}} = \Sigma X_{\text{ads}} - \Sigma X_{\text{reg}}), \quad \text{which}$$

with 2 % of error allows choosing  $w_k$  values in order to reach methanol oxidation degree from 92 % to 95 %. It was calculated from equation that such values of oxidation degree would be reached if adsorbent-catalyst would be heated at 67–70 °C/(cm min) rate.

The maximum working temperature of adsorbent-catalyst is about 500 °C. Reaching this temperature catalyst loses carbon inserts: specific surface area  $S_{BET}$  decreases from 244.7 m<sup>2</sup>/g to 16.45 m<sup>2</sup>/g.

#### 4. CONCLUSIONS

Thermostable up to about 500 °C Al<sub>2</sub>O<sub>3</sub>-C<sub>act</sub>-(CuO, Cr<sub>2</sub>O<sub>3</sub>, Co<sub>3</sub>O<sub>4</sub>) adsorbents-catalysts were obtained using sol-gel technology. At higher temperatures activated carbon is lost. The best samples have 5 % of activated carbon, 6.8 % CuO, 3.1 % Cr<sub>2</sub>O<sub>3</sub> and 2.0 % Co<sub>3</sub>O<sub>4</sub>.

The specific surface area of Al<sub>2</sub>O<sub>3</sub>-C<sub>act</sub>-(CuO, Cr<sub>2</sub>O<sub>3</sub>, Co<sub>3</sub>O<sub>4</sub>) adsorbent-catalyst depends on the amount of WS-42A activated carbon. It was found that  $S_{BET} = 244.7$  m<sup>2</sup>/g. The system is mesoporous, as 1.8 nm–2.0 nm and 2.4 nm–2.7 nm radius pores prevail and their total volume is  $\Sigma V_p = 0.652$  cm<sup>3</sup>/g.

Oxidation degree of methanol depends on heating rate of Al<sub>2</sub>O<sub>3</sub>-C<sub>act</sub>-(CuO, Cr<sub>2</sub>O<sub>3</sub>, Co<sub>3</sub>O<sub>4</sub>) adsorbent-catalyst bed. At 400 °C–420 °C when heating rate  $w_k = (67–70)$  °C/(cm min), the methanol oxidation degree reaches 92 %–95 %.

#### REFERENCES

1. Serp, P., Figueiredo, J. L. Carbon Materials for Catalysis. New Jersey: Wiley, 2009: 579 p.
2. Radovic, L. R. Chemistry and Physics of Carbon. Vol. 29. CRC Press, 2004: 448 p. <http://dx.doi.org/10.1201/9780203997031>
3. Marsh, H. Activated Carbon Compendium. Elsevier Science, 2001: 297 p.
4. Erti, G., Knozinger, H., Schuth, F., Watkamp, J. Handbook of Heterogeneous Catalysis, Vol. 1. 2<sup>nd</sup> Ed. Weinheim: Wiley-VCH, 1997: 2479 p.
5. Oloncev, V. F. Some Tendencies of Production and Application of Activated Carbons in the World *Chemical Industry* 8 2000: pp. 7–14 (in Russian).
6. Kuznetsov, B. N. Carbon Sorbents Synthesis and Application *Soros Educational Journal* 12 1999: pp. 29–34.
7. Likhoholov, V. A., Felonov, V. B., Okkel, L. G. et al. New Carbon-Carbonaceous Composites For Catalysis And Adsorption *Reaction Kinetics and Catalysis Letters* 54 (2) 1995: pp. 381–411. <http://dx.doi.org/10.1007/BF02071033>
8. Likhoholov, V. A. Catalytic Synthesis of Carbon Materials and Their Application in Catalysis *Soros Educational Journal* 5 1997: pp. 35–42.
9. Elvers, B., Hawkins, S., Russey, W. Ullman's Encyclopedia of Industrial Chemistry. Vol. A5. New York, 1986: 556 p.
10. Fidalgo, B., Menendez, J. A. Carbon Materials as Catalysts for Decomposition and CO<sub>2</sub> Reforming of Methane: A Review *Chinese Journal of Catalysis* 32 (2) 2011: pp. 207–216. [http://dx.doi.org/10.1016/S1872-2067\(10\)60166-0](http://dx.doi.org/10.1016/S1872-2067(10)60166-0)
11. Gaur, V., Sharma, A., Verma, N. Catalytic Oxidation of Toluene and m-xylene by Activated Carbon Fiber Impregnated with Transition Metals *Carbon* 43 2005: pp. 3041–3053.
12. Gaur, V., Sharma, A., Verma, N. Removal of SO<sub>2</sub> by Activated Carbon Fibre Impregnated with Transition Metals *The Canadian Journal of Chemical Engineering* 85 2007: pp. 188–198.
13. Chuang, K-H., Liu, Z-S., Wey, M-Y. Catalytic Activity of Cooper-supported Catalyst for NO Reduction in the Presence of Oxygen: Fitting of Calcination Temperature and Copper Loading *Materials Science and Engineering* 175 2010: pp. 100–107.

14. **Illan-Gomez, M. J., Linares-Solano, A., Radovic, L. R., Salinas-Martinez de Lecea, C.** NO Reduction by Activated Carbons. 7. Some Mechanistic Aspects of Uncatalyzed and Catalyzed Reaction *Energy & Fuels* 10 1996: pp. 158–168.  
<http://dx.doi.org/10.1021/ef950066t>
15. **Lu, Ch-Y., Wey, M-Y.** Simultaneous Removal of VOC and NO by Activated Carbon Impregnated with Transition Metal Catalysts in Combustion Flue Gas *Fuel Processing Technology* 88 2007: pp. 557–567.
16. **Zaman, M., Khodadi, A., Mortazavi, Y.** Fischer-Trosch synthesis over cobalt dispersed on Carbon Nanotubes-based Supports and Activated Carbon *Fuel Processing Technology* 90 2009: pp. 1214–1219.
17. **Lee, J. J., Han, S., Koh, J. H., Hyeon, T., Moon, S. H.** Performance of CoMoS Catalysts Supported on Nanoporous Carbon in the Hydrodesulfurization of Dibenzothiophene and 4,6-Dimethyldibenzothiophene *Catalysis Today* 86 2003: pp. 141–149.  
[http://dx.doi.org/10.1016/S0920-5861\(03\)00408-5](http://dx.doi.org/10.1016/S0920-5861(03)00408-5)
18. **Stankova, N. B., Khristova, M. S., Mehandjiev, D. R.** Catalytic Reduction of NO with CO on Active Carbon-supported Copper, Manganese, and Copper-manganese Oxides *Journal of Colloid Interface Science* 241 2001: pp. 439–447.
19. **Bashkova, S., Baker, F. S., Wu, X., Armstrong, T. R., Schwartz, V.** Activated Carbon Catalyst for Selective Oxidation of Hydrogen Sulphide: On the Influence of Pore Structure, Surface Characteristics and Catalytically-active Nitrogen *Carbon* 45 (6) 2007: pp. 1354–1363.
20. **Miguel, S. R., Roman-Martinez, M. C., Cazorla-Amoros, D., Jablonski, E. L., Scelza, O. A.** Effect of the Support in Pt and PtSn Catalysts Used for Selective Hydrogenation of Carvone *Catalysis Today* 66 (2–4) 2001: pp. 289–295.
21. **Spassova, I., Velichkova, N., Khristova, M., Georgescu, V.** NO Reduction with CO on Cu–Cr and Co–Cr Oxide Catalysts Supported on Al<sub>2</sub>O<sub>3</sub> and Al<sub>2</sub>O<sub>3</sub>+SiO<sub>2</sub> *Reaction Kinetics, Mechanisms and Catalysis* 101 2010: pp. 321–330.  
<http://dx.doi.org/10.1007/s11144-010-0229-4>
22. **Lindstrom, B., Petterson, L. J., Govind Menon, P.** Activity and Characterization of Cu/Zn, Cu/Cr and Cu/Cr on  $\gamma$ -alumina for Methanol Reforming for Fuel Cell Vehicles *Applied Catalysis A: General* 234 2002: pp. 111–125.  
[http://dx.doi.org/10.1016/S0926-860X\(02\)00202-8](http://dx.doi.org/10.1016/S0926-860X(02)00202-8)
23. **Zhu, H., Shen, M., Gao, F., Kong, Y., Dong, L., Chen, Y., Jian, C., Liu, Z.** A Study of CuO/CeO<sub>2</sub>/Al–Zr–O in “NO+CO” *Catalysis Communications* 5 2004: pp. 453–456.  
<http://dx.doi.org/10.1016/j.catcom.2004.05.010>
24. **Park, P. W., Ledford, J. S.** Characterization and CO Oxidation Activity of Cu/Cr/Al<sub>2</sub>O<sub>3</sub> Catalysts *Industrial and Engineering Chemistry Research* 37 1998: pp. 887–893.  
<http://dx.doi.org/10.1021/ie970494h>
25. **Pantaleo, G., Liotta, L. F., Venezia, A. M., Deganello, G., Ezzo, E. M., El Kherbawi, M. A., Atia, H.** Support Effect on the Structure and CO Oxidation Activity of Cu–Cr Mixed Oxides over Al<sub>2</sub>O<sub>3</sub> and SiO<sub>2</sub> *Materials Chemistry and Physics* 114 2009: pp. 604–611.  
<http://dx.doi.org/10.1016/j.matchemphys.2008.10.006>
26. **Kirpšaitė, E., Dabrilaitė-Kudžmienė, G., Kitrys, S.** Al<sub>2</sub>O<sub>3</sub>-C<sub>act</sub> Derivatives: Synthesis and Properties *Materials Science (Medžiagotyra)* 16 (4) 2010: pp. 353–358.
27. **Brazlauskas, M.** Sandwich Type CuO/(NaA, NaX, CaA, CaX) Adsorbents-Catalysts: Synthesis and Properties *Summary of Doctoral Dissertation* Kaunas, 2009.
28. **Baron, N. M.** Short Handbook of Physicochemical Quantities. Sankt Peterburg, 1999: 512 p.
29. **Yilmaz, S., Kutmen-Kalpakli, Y., Yilmaz, E.** Synthesis and Characterization of Boehmitic Alumina Coated Graphite by Sol-gel Method *Ceramics International* 35 (5) 2009: pp. 2029–2034.
30. **Sun, Z.-X., Zheng, T.-T., Bo, Q.-B., Du, M., Forsling, W.** Effects of Calcination Temperature on Pore Size and Wall Crystalline Structure of Mesoporous Alumina *Journal of Colloid and Interface Scienc* 319 2008: pp. 247–251.
31. **Guo, X., Liu, X., Xu, B., Dou, T.** Synthesis and Characterization of Carbon Sphere-silica Core-shell Structure and Hollow Silica Spheres *Colloids and Surfaces A* 324 (1–3) 2009: pp. 141–146.
32. **Brown, M. E.** Introduction to Thermal analysis: Techniques and Applications. New York: Springer, 2001: 280 p.
33. **Kitrys, S., Dabrilaitė, G.** Synthesis and Surface Area Analysis of Al<sub>2</sub>O<sub>3</sub>-activated carbon Adsorbent *Chemical Technology (Cheminė Technologija)* 5 (26) 2002: pp. 26–30 (in Lithuanian).
34. **Thomas, J.** Methods for Studying Catalysts. Moscow, 1983: 304 p.
35. **Greg, S., Sing, K.** Adsorption Surface Area and Porosity. Moscow, 1984: 306 p.
36. **Orr, C., DallaValle, J. M.** Fine Particle Measurements. New York: Macmillan, 1959: 271 p.
37. **Alchasov, T. G., Margolis, L. Y.** Deep Oxidation of Organic Compounds. Moscow, 1985: 192 p.